Design and development of a multi-modal aerial-ground vehicle for long-endurance inspection applications

Teodoro Afonso de Sousa Clemente Pinto Dias
Department of Electrical and Computer Engineering, Instituto Superior Tecnico, Lisbon, Portugal
Supervisor: Dr. Meysam Basiri

***Abstract*—During the last decade, the use of Micro Aerial Vehicles (MAVs) in applications such as inspection and surveillance has proved to be extremely useful. However, the usability of these vehicles is negatively impacted by the large power requirements of flight, limited payload and operating time. On the other hand, ground vehicles are able to transport larger payloads and have a higher operating time, being limited by their capacity to overcome obstacles in their path. Thus, applications in which both types of robots are used in combination have started to emerge. This work describes the design and development of a hybrid aerial-ground vehicle, BogieCopter, enabling multi-modal mobility in challenging terrains, enabling the locomotion in potentially cluttered and narrow spaces, and having a higher operating time when compared to aerial-only vehicles. The design consists of a MAV with two tiltable axles and four independent passive wheels, allowing the vehicle to fly, approach, land and move on flat and inclined surfaces. In comparison to existing multi-modal vehicles with passive actuated wheels, the design of BogieCopter enables a higher ground locomotion efficiency, provides a higher payload capacity suitable for inspection applications, and presents one of the lowest mass increases due to the ground actuation mechanism. Furthermore, the vehicle's performance is evaluated through a series of real experiments, demonstrating its flying, ground locomotion and wall-climbing capabilities. Finally, the energy consumption for different modes of locomotion is demonstrated.**

***Index Terms*—Aerial-Ground Locomotion, Inspection Applications, Micro Aerial Vehicles, Multi-Modality, Prototype Design and Development**

I. Introduction

During the last decade, Unmanned Aerial Vehicles (UAVs), especially Micro Aerial Vehicles (MAVs), have been perceived with increasing interest, both academically as commercially, due to their ability to quickly reach a desired location, to overcome obstacles, and to provide a bird's-eye view of the environment. The applications which use MAVs have been multiplying throughout the years, and include crop evaluation [1], inspection applications [2], package delivery [3], search and rescue [4] and surveillance [5]. Despite the benefits gained from the use of MAVs in these applications, their use is heavily impacted by the lack of capability to remain airborne for an extended period of time, due to the high power requirements of flight, and by the low payload capacity that these vehicles possess. On the other hand, ground vehicles (GVs) excel in their energy efficiency, payload capacity, and ability to move in narrowed and constrained spaces.

Trying to combine the benefits of both types of vehicles, research has been conducted in which a MAV is used together with a GV to cooperatively perform a task [6], [7]. The MAV is used to rapidly identify a problem or a target [7], or to overcome an obstacle [6], while the GV performs the majority of the task. Multi-modal MAVs have been gaining attention in some of these applications in which two different types of robots were used. These combine the ability of aerial locomotion with, usually, the ability of ground locomotion in a single hybrid vehicle.

Prior work largely falls into two categories depending on whether the ground mode is active or passive actuated. In passive actuated designs, the same actuators used for flight enable the MAV to move on the ground, while in active actuated designs, additional actuators are added, usually electric motors, for the ground locomotion. Table I presents the prior work, both commercial and academic, as well as some characteristics that are of interest in multi-modal vehicles. It can be determined that most of these vehicles can't be considered fit to be used in more than the designed use case since, in most of the designs, details such as the payload aren't specified and low Thrust-to-Weight ratios (T/W ratios) are used. With the T/W ratios used, the vehicle's thrust does not have a high enough safety factor (SF) [8] for it to be considered safe to fly in windy conditions. It is also possible to demonstrate the advantages of a hybrid design in terms of the operating time of the vehicle, with the addition of a ground actuation mechanism increasing it by a minimum of 1.33x and a maximum of 11.25x. The minimum mass achieved for the ground actuation mechanism in terms of the maximum take-off mass (MTOM) is 1.03%, by Gemini [9], [10]. However, it requires active actuation to be static on the ground, having a power consumption of 106 W. Considering only designs that don't require energy to be static on flat surfaces, the lowest mass attained for the ground actuation mechanism, with respect to the MTOM, is 11.8%, by [11]. It should be noted that [12] and [13] don't focus on the development of a multi-modal MAV, but instead focus on the capability of the MAV to move in contact with walls, with the design enabling the vehicle to move on flat and planar surfaces. To the best of our knowledge, to the exception of [13] (which doesn't implement ground locomotion) and [14], the design of the passive actuated multi-modal MAVs requires the use of dependent and coupled flight and ground controllers, reducing the ability to optimize them [15]. Also, to the best of our knowledge, to the exception of [14], the passive actuated multi-modal MAVs use the same similar inefficient ground actuation mechanism.

A. Novel Contribution

This work addresses some of the existing limitations of multi-modal MAVs, by introducing BogieCopter, a four-

MAV	Main Use Case	Payload	Maximum Take-off Mass (MTOM)	Thrust-to-Weight Ratio	Type of Ground Actuation	Ground Mechanism Mass compared to MTOM (%)	Ground Operating Time[1]
Pegasus [5]	Surveillance	NS[2]	NS	NS	Active	NS	NS
B-Unstoppable [16]	Hobby	NS	NS	NS	Active	NS	$>$ 1.33x
[17]	NS	NS	946 g[3]	NS	Active	NS	NS
WAMORN [18]	Disaster Sites	NS	350 g	$\sim$ 1.06	Active	NS	NS
[19]	Crop Evaluation	NS	NS	NS	Active	NS	$<$ 1.75x
[12]	Inspection	NS	NS	NS	Active	NS	NS
MTMUR [20]	NS	NS	1.5 kg[3]	$\sim$ 3.4	Active	NS	NS
Drivocopter [15]	DARPA SubT Challenge	850 g	5.1 kg	NS	Active	$\sim$ 17.6	$\sim$ 11.25x
JJRC H3 [21]	Hobby	NS	NS	NS	Active	NS	NS
Syma X9 [22]	Hobby	NS	NS	NS	Active	NS	NS
HyTAQ [23], [24]	NS	NS	570 g[3]	$\sim$ 2.36	Passive	NS	$\lesssim$ 6x
[25]	Bridge Inspection	$\geq$ 74 g	1.36 kg[3]	NS	Passive	NS	NS
MUWA [26]	Disaster Sites	NS	2.1 kg	$\sim$ 2.16	Passive	NS	NS
PRSS UAV [27]	Disaster Sites	$\geq$ 76 g	2kg	$<$ 1.5	Passive	$\sim$ 33.2	NS
Rollocopter [28]	Space Exploration	NS	NS	NS	Passive	NS	NS
Shapeshifter [29], [30]	Space Exploration	NS	$\sim$ 800 g	$\sim$ 4.08	Passive	NS	NS[5]
Gemini [9], [10]	Confined Spaces	500 g	1.95 kg[3]	$\sim$ 1.28	Passive	$\sim$ 1.03	$\lesssim$ 2.58x
NINJA UAV [31]	NS	NS	2.122 kg[3]	NS	Passive	NS	NS
Rollocopter [11]	NS	850 g[4]	4.231 kg	$\sim$ 1.47	Passive	$\sim$ 11.8	$\sim$ 5
Parrot Rolling Spider [32]	Hobby	NS	NS	NS	Passive	NS	NS
Flying STAR [14]	Confined Spaces	NS	900 g[3]	$\sim$ 1.36	Passive	NS	NS
Inkonova Tilt Scout [33]	Subterranean Inspection	300 g	NS	NS	Passive	NS	NS
Quadroller [34]	NS	NS	1.3 kg[3]	NS	Passive	$\sim$ 22.3	$\sim$ 2
Bi[2]Copter [13]	Bridge Inspection	$\sim$ 2.34 kg	$\sim$ 4.84 kg	$\sim$ 1.26	Passive	NS	NS

[1] Increase when compared to flight operating time [2] Not Specified [3] Unknown if it is higher [4] Similar payload to [15]
[5] Presented theoretical operating ranges

TABLE I
CHARACTERISTICS OF INTEREST OF THE DIFFERENT REVIEWED MULTI-MODAL ROTARY-WING MAVS

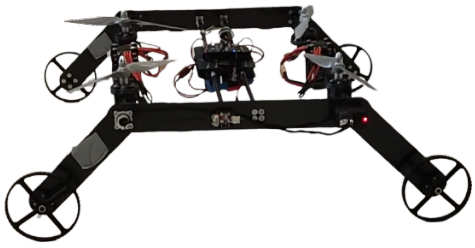

Fig. 1. BogieCopter

wheeled single-axis dual tiltable quadrotor, shown in figure 1. Our work differs from prior work in hybrid aerial-ground vehicles since we draw from the strengths of both active and passive ground actuation mechanisms, while taking into consideration the payload required for most of the industrial applications in which MAVs are used. The developed MAV was designed from the ground up as being passive actuated, due to the lower impact that the mass of this type of ground actuation mechanism has in the MTOM of the vehicle. By using tilt-rotors, BogieCopter decouples the ground from the flight controller, and is capable of efficient ground locomotion and wall-climbing. Furthermore, the design takes into consideration the protection of the propellers, acting as a cage around them, providing similar protection as that provided by caged designs, without the negative impact on the, possible used, vision and perception systems.

In the following sections, a detailed overview and explanation of the hybrid aerial-ground vehicle are provided. This document starts by presenting the theory of a rotor system, and deriving the equations of motion for the vehicle, in Section II. In Section III, the limitations of existing passive actuated multi-modal MAVs are discussed and the proposed MAV, with a dual connected bi-copter design, is described. The actual vehicle developed is presented in Section IV. In Section V, the design is validated through multiple real test scenarios, validating the performance of BogieCopter through flight and

ground locomotion test, on flat and inclined surfaces, and through an analysis of the power consumption of the vehicle at different operating states. Finally, Section VI concludes the document and Section VII presents the future work.

II. Theory and Dynamics Models

In this section, the theory that enables the theoretical evaluation of the performance of the rotors is presented as are the dynamic models for the different modes of locomotion of the vehicle.

A. Rotor Performance

A rotor is constituted by a motor and a propeller. To evaluate the performance of a rotor, it is necessary to evaluate the performance of the motor and of the propeller. Here we are only going to focus on the performance of the propellers, since it enables an approximation of the real performance of the rotors. We are interested in presenting some conclusions that can be arrived at by using the momentum theory [35], influencing the choice of the propulsive system.

The propeller uses mechanical power to accelerate the air going through the propeller's disk area, corresponding to the area covered by the rotating propeller. The thrust and power of a single propeller, in the hovering state, can be determined by applying the Rankine–Froude model to the rotor flow [35]:

$$T = 2\rho A {v_i}^2 = \rho \frac{\pi}{2} D^2 {v_i}^2 \tag{1}$$

$$P = T v_i = T\sqrt{\frac{T}{2\rho A}} = \sqrt{\frac{T^3}{\rho \frac{\pi}{2} D^2}} \tag{2}$$

Where T is the thrust produced by the propeller [N]; ρ is the medium density [kg/m^3]; A is the area covered by the rotating propeller; v_i is the induced velocity in the rotor plane [m/s]; D is the propeller diameter [m]; P is the power [W].

Analysing equation 1, we can determine that T increases when D or ρ increase. This influence of ρ in T is what greatly influences the altitude that rotary-wing vehicles can achieve. We can also conclude that increasing the rotational velocity of a fixed size propeller, increases the thrust produced by the propeller.

Analysing equation 2, it is possible to verify that $P \propto T^{\frac{3}{2}}$ and $P \propto \frac{1}{D^2}$. This implies that P has an exponential relation with T and that, to achieve the highest possible propeller efficiency (highest T with lowest P), D should be as large as possible.

For a co-axial rotor system, we can determine that the power required for the propellers, $P_{co-axial}$ is given by [35]:

$$P_{co-axial} = 2T(v_i)_{system} = \frac{(2T)^{\frac{3}{2}}}{\sqrt{2\rho A}} \tag{3}$$

Comparing the power required by a co-axial rotor (equation 3) with the power required by two single non-interacting propellers, we get:

$$\frac{P_{co-axial} - P_{2rotors}}{P_{2rotors}} = \frac{\left(\frac{(2x)^{\frac{3}{2}}}{\sqrt{2yz}} - \frac{2(x)^{\frac{3}{2}}}{\sqrt{2yz}}\right)}{\frac{2(x)^{\frac{3}{2}}}{\sqrt{2yz}}} = 0.414 \tag{4}$$

From equation 4 it is possible to verify that co-axial rotors require 41.4% more power to produce the same thrust as the two single non-interacting propellers, $P_{2rotors}$. Experiments have shown that this value is lower, corresponding to, approximately, 16% [35]. Due to this higher power requirement of co-axial rotors, their use requires an extensive study of the interaction between wakes in order to keep this increase as low as possible [36].

B. Aerial Mode Dynamic Model

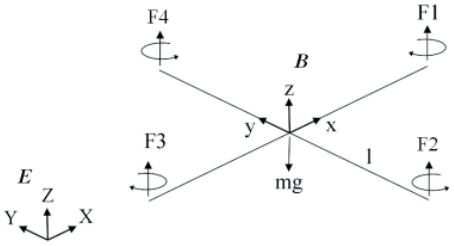

Fig. 2. Usual coordinate frame system used to derive the dynamics of quadrotors [37] (Earth fixed or inertial frame and body frame represented by the letter E and B, respectively)

In flight, BogieCopter behaves just like a regular quadrotor, being that the addition of the ground actuation mechanism only changes the mass and the moments of inertia of the vehicle. The dynamics of such systems have already been derived in multiple articles [37], [38] and are only summarized here.

Using the reference frames presented in figure 2, the equations of motion for a quadrotor during flight are given by:

$$m_B \cdot {}^E\ddot{\mathbf{r}}^{B^*} = -m_B \mathbf{g} + u_f \widehat{\mathbf{z}} - u_d \cdot \frac{{}^E\dot{\mathbf{r}}^{B^*}}{\left\| {}^E\ddot{\mathbf{r}}^{B^*} \right\|} \tag{5}$$

$$\mathbf{I}^B_{B^*} \cdot {}^E\dot{\boldsymbol{\omega}}^B = \begin{bmatrix} u_\phi \\ u_\theta \\ u_\psi \end{bmatrix} - {}^E\boldsymbol{\omega}^B \times \mathbf{I}^B_{B^*} {}^E\boldsymbol{\omega}^B \tag{6}$$

Where m_b is the vehicles' mass; B^* represents the frame in the center of mass (CoM) of the vehicle; ${}^E\mathbf{r}^{B^*}$ is the position vector from a fixed point in the earth fixed frame to the CoM of the vehicle; $\mathbf{g}$ is the gravity vector; u_f is the net force along the $\widehat{\mathbf{z}}$ axis; u_d is the magnitude of the drag force; $\mathbf{I}^B_{B^*}$ is the vehicle's moment of inertia about its CoM, along the $\widehat{\mathbf{x}}$, $\widehat{\mathbf{y}}$, and $\widehat{\mathbf{z}}$ axes; ${}^E\boldsymbol{\omega}^B$ is the Earth-observed rotational velocity of body frame, $\mathbf{B}$; ϕ, θ, and ψ are the Euler angles specifying the vehicle's attitude; u_ϕ, u_θ, and u_ψ are the propellers' induced moments along the $\widehat{\mathbf{x}}$, $\widehat{\mathbf{y}}$, and $\widehat{\mathbf{z}}$ axes, respectively.

C. Ground Mode Dynamic Model

The ground locomotion of BogieCopter is enabled by its ground mechanism, which is composed by four independently rotating passive actuated wheels, and by the use of tilt rotors, enabling the thrust produced to be parallel to the surface where

it moves. With these characteristics, it can be assumed that the vehicle behaves just like a differential drive mobile robot (DDMR) in which the forces aren't applied by the wheels but are by the rotors. The dynamics of such systems have already been derived in multiple articles [39], [40], [41] and are only summarized here, following [41]. The dynamics of the vehicle presented are derived with the Newton-Euler approach since we have an interest in describing the system by its forces and constraints. For the derivation of the dynamics, it is assumed that there is no lateral slip motion, each wheel maintains one contact point with the ground, and the vehicle is considered as one rigid body.

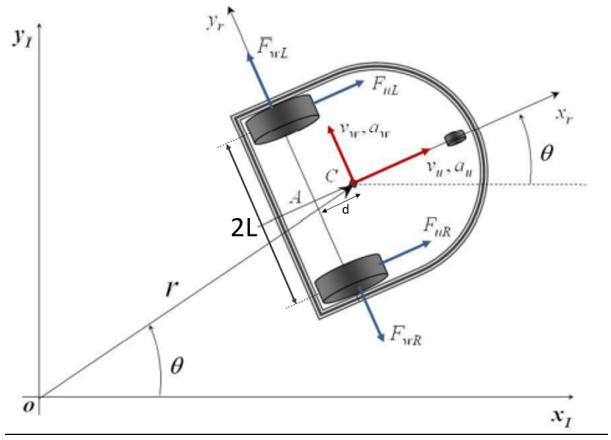

Fig. 3. Differential drive mobile robot (DDMR) free body diagram for Newtonian dynamic modeling, with forces represented. Adapted from [41]

Figure 3 present the free body diagram of a DDMR and the forces acting on it. Using the vehicle body frame $[x_r, y_r]$: v_u and v_w represent the longitudinal and the lateral velocity, respectively, of the vehicle's CoM (C) in its body frame; a_u and a_w are the longitudinal and the lateral accelerations, respectively, of the vehicle's CoM in its body frame; F_{u_r} and F_{u_l} are the longitudinal forces exerted on the vehicle by the right and left wheels, respectively; F_{w_r} and F_{w_l} are the lateral forces exerted on the vehicle by the right and left wheels, respectively; θ is the vehicle's orientation; m is the vehicle's mass; I is the vehicle's moment of inertia about its CoM, in its body frame; d is half the vehicle's wheelbase; L is half the vehicle's trackwidth.

Applying the Newton-Euler approach, the following equations of motion are obtained for the DDMR [41]:

$$\dot{v_u} = d\dot{\theta}^2 + \frac{1}{m}(F_{u_R} + F_{u_L}) \tag{7}$$

$$\ddot{\theta} = \frac{L}{md^2 + I}(F_{u_R} - F_{u_L}) - \frac{mdv_u}{md^2 + I}\dot{\theta} \tag{8}$$

We can transpose the dynamics obtained in equations 7 and 8 for a vehicle that has wheels but isn't actuated by them, being propelled by rotors, as the case of BogieCopter. The requirement is that the rotors should be distanced from the vehicle's CoM, longitudinally, by d and, laterally, by L. Considering the rotors are parallel to the ground and that the vehicle is actuated by two rotors, while still having independent passive wheels (we can imagine the DDMR represented in figure 3 having one supporting wheel and two rotors instead of having one supporting wheel and two actuated wheels), the thrust produced by the right and the left rotor corresponds to F_{u_R} and F_{u_L}, respectively.

III. Passive Actuated Multi-modal MAVs

Passive actuated multi-modal MAVs commonly use a similar design that results in inefficient ground mode locomotion. In this section, an explanation for this inefficiency is provided and a design that enables a more efficient ground locomotion is presented.

A. Issues of Conventional Passive Actuated Designs

In the common passive actuated multi-modal MAV design, the longitudinal locomotion of the vehicle is enabled by the pitching of the MAV and the control of its thrust, as represented in figure 4.

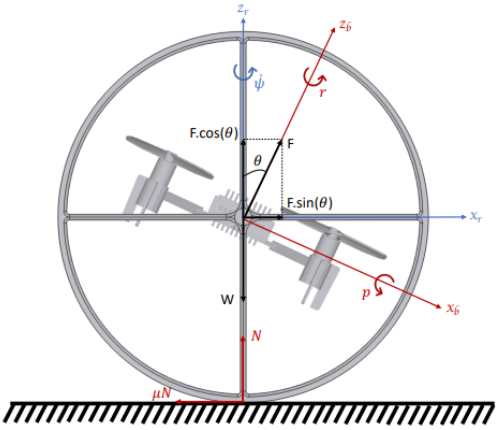

Fig. 4. Conventional passive actuated design, with the longitudinal motion enabled by the pitching of the MAV [42]

This requirement that the vehicle needs to be able to pitch while on the ground, constraints the design of the vehicle, requiring the MAV to be mounted on a single axle, connected to the mechanism that enables the ground locomotion (wheels, for example). This is the reason why rolling cage and two-wheeled designs are so common in passive actuated designs.

The thrust produced by the MAV, while pitching, can be decomposed into two forces, one perpendicular and the other parallel to the ground. Using the notation from figure 4, we can determine:

$$F_{\parallel} = F\sin(\theta) \tag{9}$$

$$F_{\perp} = F\cos(\theta) \tag{10}$$

Where F is the total thrust produced by the MAV; $F_{\parallel}$ and $F_{\perp}$ are the components of the thrust parallel and perpendicular to the surface plane, respectively; θ is the pitching angle of the MAV.

Only $F_{\parallel}$ is responsible for the longitudinal motion of the MAV, with $F_{\perp}$ only impacting the normal force and the rolling resistance. We can conclude that, to extend the operating time of the vehicle while moving on the ground, $F_{\parallel}$ should be maximized and $F_{\perp}$ minimized, implying that the vehicle should

move at a pitch angle of 90°. This is the same conclusion that was arrived at [24]. This result can be broadened to inclined surfaces. For the MAV to move efficiently on inclined surfaces, with slope angles up to, and including, 90°, the pitch angle of the MAV should be equal to:

$$\theta = 90° - \psi \tag{11}$$

Where ψ is the slope angle. In the common passive actuated multi-modal MAV design, for this more efficient locomotion on inclined surfaces, an *a priori* knowledge of the slope may be required [42]. Additionally, this relation between the pitch angle and the ground longitudinal motion of the vehicle implies that the flight and ground controller are coupled [15], not allowing to, independently, optimize them.

B. BogieCopter Passive Actuated Design

BogieCopter design addresses the previously mentioned issues from the conventional design of passive actuated multi-modal MAVs. For an efficient ground locomotion, the thrust produced by the rotors should be parallel to the surface plane. For the rotors to be parallel to flat surfaces during ground locomotion and perpendicular for flight (as in common multirotors), a tilt rotor mechanism is required. In order for the MAV to be able to accelerate and decelerate while moving on the ground (propellers used only produce thrust in one direction), a dual tilt axle mechanism is required, which tilts the rotors assembled in different axles (two rotors per axle) in opposite directions. This is the principle behind the design of BogieCopter, as presented in figure 5.

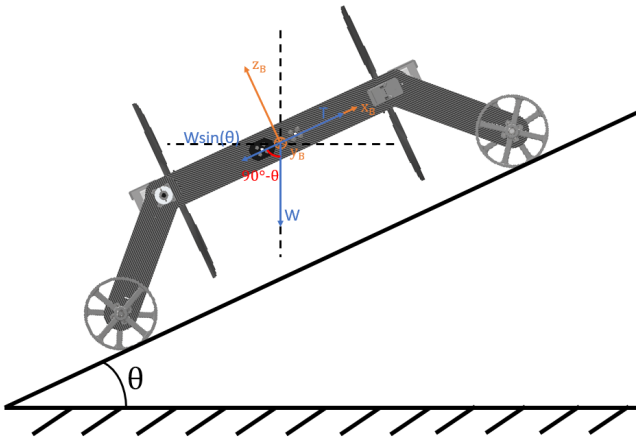

Fig. 5. BogieCopter climbing an inclined surface, showing the rotor position and the forces acting on it (normal force and friction not represented)

By using a dual connected bi-copter design (as referred in [13]), the passive actuated design is no longer constrained by the assembly of the MAV on an axle, enabling the use of a four-wheel design, which is, inherently, a more stable design. This also enables the decoupling between the ground and the flight controller. By tilting the rotors 90°, an efficient ground locomotion is achieved, in the sense that there is no thrust being misapplied in other functions other than the longitudinal motion of the vehicle. Besides, *a priori* knowledge of the slope of the inclined surface isn't required for the efficient locomotion, since the rotors are always parallel to the surface. Additionally, we can determine that F_{u_R} and F_{u_L}, from equations 5 and 6, are given by the resultant force between the produced thrust of the two rightmost and left most rotors, respectively. Furthermore, the use of tilting rotors can enable the vehicle to wall-climb [12], hover at any given pitch angle [13], and can enable a more efficient forward flight [43], advantages that can have benefits for many applications.

IV. BogieCopter Design Overview

BogieCopter was designed as being a cost-effective platform, easily upgradeable and easily manufactured, being that all the custom parts can be constructed with only a 3D printer.

A. Hardware

The design of an aerial vehicle is an iterative process due to the interdependency between the several components that compose the vehicle [44]. The design process has already been presented in numerous publications [44], [45], [46], being only summarized here. The design begins by setting three design constraints: the maximum take-off mass (MTOM), maximum vehicle span, and the T/W ratios.

The maximum vehicle span considered was equal to the size of commonly available quadrotors used for outdoor industrial applications (DJI Flamewheel F450 frame [47] with the use of propeller guards), corresponding to 700 mm. A rule of thumb in the design of multirotors is that the T/W ratio should be equal to two [20], [23], [46], providing a factor of safety for the thrust that the vehicle is able to produce, enabling the multirotor to be used in windy conditions. The MTOM was estimated from the payload that the vehicle should be able to carry. Considering inspection applications, namely the inspection of photovoltaic solar panels, the sensors most commonly are RGB and thermal cameras, and LIDARs. Adding a SF to the mass estimated for the previously mentioned sensors, the payload was estimated to be 2 kg. From the payload, the total vehicle's mass (propulsive system, frame, passive actuated ground mechanism) was estimated to also be 2 kg and the MTOM to be 4 kg.

Having estimated these three parameters, it is possible to select the propulsive system, which makes use of single rotors, due to the inefficiency of co-axial rotors, as illustrated in equation 4. To have the highest possible efficiency, propellers with the largest possible diameter should be used. Due to size constraints of the vehicle, this limits the propeller to a maximum diameter of 254 mm. The propellers analysed for the propulsive system were limited to APC, due to the availability of simulated data for their propellers [48]. The propellers were analysed using a custom script, which constrained the propellers by their dimension, maximum thrust and efficiency, reducing the available number of propellers from 526 to 17. From these, the selected propeller was the APC 10x5E. Having selected the propeller, it was possible to select the motor. The available motors were constrained by weight, availability, the existence of performance charts, and their efficiency in those performance charts (if they existed). The selected motor was the T-Motor AT2814. Having selected the rotor system, it

was possible to estimate a power consumption for the hover state. Due to the design of BogieCopter, which makes use of two batteries in the propulsive system, the battery selected was Li-po 4S with 5 Ah, providing a total of 14 minutes of hovering time for the MTOM. The MAV also uses an independent battery to power its electronics, which is a Li-ion 2S 3.2 Ah battery. The servos selected needed to have a torque higher than the gyroscopic moment of the rotating propellers [20], [49], in order to be able to rotate the bi-copter modules, had to provide full 360º resolution, and be lightweight. The chosen servos were the Feetech RC STS3215. The autopilot used is a Pixhawk 1. Due to the challenges that the use of this autopilot presents with the use of three batteries, two custom made PCBs were designed, the SmartBat and the SmartBat and Router, which communicate the instantaneous current and individual cell voltages of the batteries through I^2C/TWI, and control the state of charge (SoC) of the cells, to protect them from over-discharge. The PCBs act as simple smart batteries and implement some of the specifications of the SMBus protocol [50]. Besides these two PCBs, a simple harnessing router PCB was also designed, the Lateral Router. Figure 6 depict the custom made PCBs. An overview of the electronic design and the harnessing is presented in figure 7

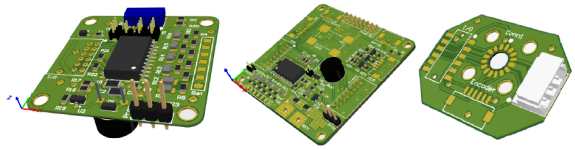

Fig. 6. Custom made PCBs, from the left to the right: SmartBat and Router, SmartBat and Lateral Router

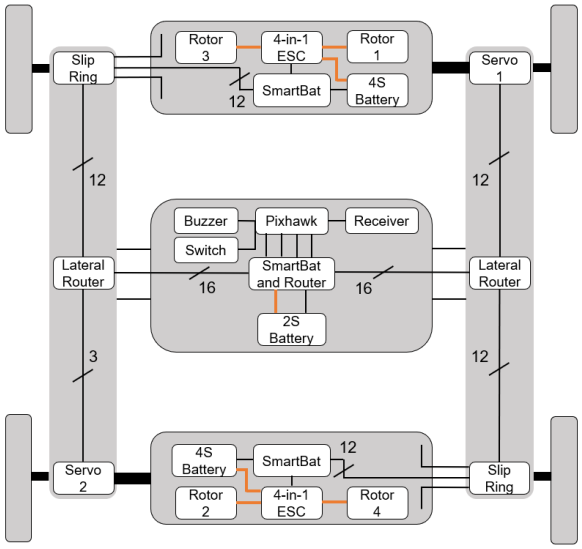

Fig. 7. Hardware and harnessing overview of BogieCopter

The mechanical design of BogieCopter was also conceptualised through an iterative process, in which the parts undergo topology optimization and were analysed through static stress analysis. To keep the design of BogieCopter as lightweight as possible, without losing strength, as many parts as possible were made out of carbon fibre reinforced plastic (CFRP) tubes and plates. The critical parts that couldn't be manufactured out of CFRP, were manufactured from aluminium 6082. The non-critical parts were manufactured by using a 3D printer and printed out of ABS. The design of BogieCopter took into consideration the protection of the propellers, being that its structure acts as a cage around them. The wheels were designed taking into consideration that the vehicle would be used in rocky soil ground but, by using other designs, BogieCopter could, potentially, be able to move on water, similar to [20]. Through the design phase, three concepts were idealized, as presented in figure 8, being that BogieCopter_3 was the selected design (being only referred to as BogieCopter throughout this work), given that it had the lowest mass, respected the maximum span, was more cost-effective (due to the wheels dimensions) and was more easily manufacturable. The name comes from the resemble of the developed MAV with a bogie.

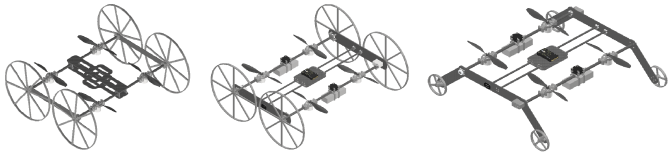

Fig. 8. The different concepts designed, from left to right: BogieCopter_1, BogieCopter_2, and BogieCopter_3

Table II summarizes the characteristics of BogieCopter and the components used.

System Overview	
Body size LxWxH	695x693.5x302 mm[1]
MTOM	4 kg
Propeller	APC 10x5E
Motor	T-Motor AT2814 1050 KV
ESC	Racerstar Air50
Propulsive System Battery	2 x Li-po 4S 5 Ah
Electronic's Battery	Li-ion 2S 3.2 Ah
Servo	Feetech RC STS3215
Autopilot	Pixhawk 1
Ground Actuation Mechanism	4x Custom Made Wheels

[1] Maximum height given when propellers are tilted parallel to the ground

TABLE II
OVERVIEW OF THE CHARACTERISTICS AND COMPONENTS OF BOGIECOPTER

B. Firmware

The firmware for BogieCopter was developed by extending the capabilities of an open-source autopilot firmware, ArduPilot [51], more precisely, those of ArduCopter. Firmware was developed to allow the use of the servos, which communicate through a protocol similar to [52], allow the use of more than one external I^2C battery monitor, which was limited to the internal bus of Pixhawk 1 and only to a single monitor, with address 0x0B, and to allow BogieCopter to be able to move on flat and inclined surfaces, just like a GV would.

C. Software

Simulation models and controllers for both BogieCopter_2 and BogieCopter were implemented in RotorS Simulator [53], enabling the development of controllers and path following

algorithms in a simulated environment. Figures 9 and 10 show the BogieCopter_2 and BogieCopter model in the Gazebo environment, hovering and on the ground, respectively.

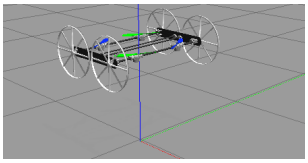

Fig. 9. BogieCopter_2 hovering, in the Gazebo environment

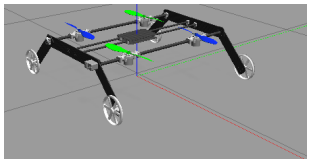

Fig. 10. BogieCopter on the ground, in the Gazebo environment

V. Experiments and Results

A. Mass

The mass of BogieCopter, without any payload, was determined to be 2.7 kg $\pm$ 0.1 kg. This value is 35% higher than what the design originally targeted. This was due to the over-dimensioning of some components, namely, the ones manufactured out of CFRP, that weren't optimized for the design load cases (a composite structure using structural foam and CFRP could have been used, instead of using solid CFRP). Still considering a MTOM of 4 kg, this means that BogieCopter is able to carry a payload of 1.3 kg $\pm$ 0.1 kg.

The ground actuation mechanism has a total mass of 328.8 g $\pm$ 0.4 g, corresponding to 8.2% of the MTOM. This is the lowest mass percentage for a multi-modal MAV that is able to be static on flat surfaces, without requiring active actuation, according to table I.

B. Rotor

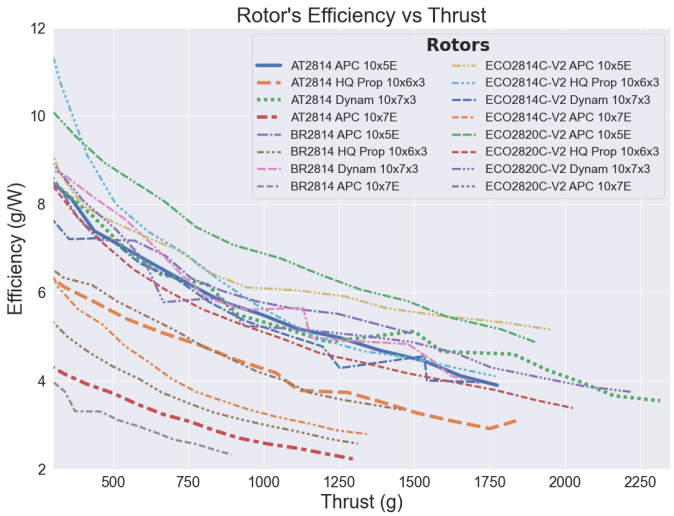

Fig. 11. Comparison between the efficiency vs thrust of different rotors. Obtained from the static thrust tests realised in a custom adapted thrust stand

Static thrust tests were conducted in a custom thrust stand, in order to validate the rotor used. The rotor was also compared with other rotors, created from four different propellers and four different motors, including the ones selected. The static thrust tests demonstrated that the selected rotor was able to produce a maximum thrust of 1.843 kg, less 7.85% than the designed maximum thrust of 2 kg. This implies that the T/W ratio of the MAV, for the MTOM, is equal to 1.843. Although being lower than two, it still provides a SF, enabling BogieCopter to operate in windy conditions. Also, to the best of our knowledge, this is the best T/W ratio among the work done in multi-modal MAVs (considering MAVs that have any payload capacity).

The static thrust tests also allowed the determination of the best rotor for BogieCopter. Figure 11 presents the efficiency in relation to thrust for all the tested rotors. From this plot, we can conclude that, by only changing the motor from the T-motor AT2814 to the Dualsky ECO2814C-V2, the operating time of the vehicle can be increased, since the latter motor is more efficient than the first, for every thrust amount.

C. Experiments

Aerial Locomotion: After building BogieCopter, the first test conducted was a flight test. The reason for this was that for flight unmodified ArduCopter firmware could be used, serving as a performance baseline. If something didn't work as intended, the build needed to be revised. From the first flight test, BogieCopter demonstrated to be a very stable and capable flying platform. Figure 12 shows a flight test of the developed MAV.

(a) (b) (c)

Fig. 12. BogieCopter flight test: (a) Climbing (b) Hovering (c) Landed

Flat Surface Locomotion: The next test phase was to, extensively, test the performance of BogieCopter while moving on flat surfaces. The first tests conducted were simple longitudinal motion tests, being followed by lateral motion tests. As a skid-steer vehicle, the developed vehicle was able to turn in place. Finally, tests that incorporated the two types of motion were realized. Figure 13 illustrates BogieCopter moving on a narrow space, with the vehicle having a clearance of 0.15 m to the walls on either side of it. While it would be almost impossible to fly a MAV in this narrow space, without the possibility of collision with the walls, it wouldn't be for a GV, such as BogieCopter in ground mode. Another test that was conducted evaluated the ground locomotion in rocky uneven soil ground, as presented in figure 14, which the multi-modal MAV was able to complete successfully.

Multi-modal Capability: The previous tests demonstrated the capabilities of BogieCopter to fly and to move on flat surfaces, but didn't demonstrated its multi-modal capabilities. A simple test was conducted in which the vehicle moves on the ground and, when faced with an obstacle, changes to aerial mode to overcome it. Once the obstacle is surpassed, the MAV can change to the more efficient ground mode locomotion. A set of images representing the test are depicted in figure 15.

Inclined Surface Locomotion: To the best of our knowl-

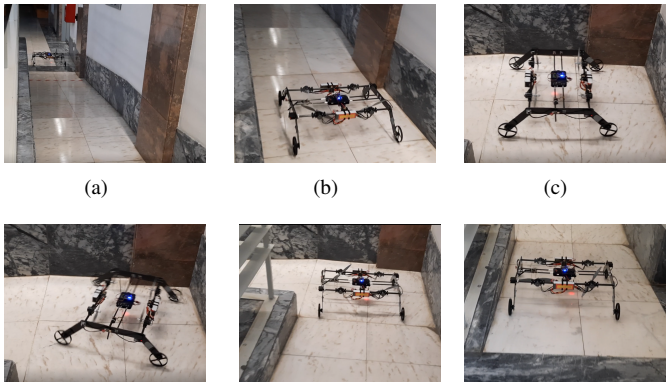

(a) (b) (c)

(d) (e) (f)

Fig. 13. Test on a long narrow wheel-chair ramp (simulated confined space: (a) Start of the test (b) Moving longitudinally (c) Arriving at a corner (d) - (e) Turning (f) Exiting the ramp

(a) (b) (c)

Fig. 14. Test on a rocky uneven soil ground: (a) Start of the test in a sidewalk (b) Moving on the rocky soil ground, moving over grass (c) Turning on the rocky soil ground

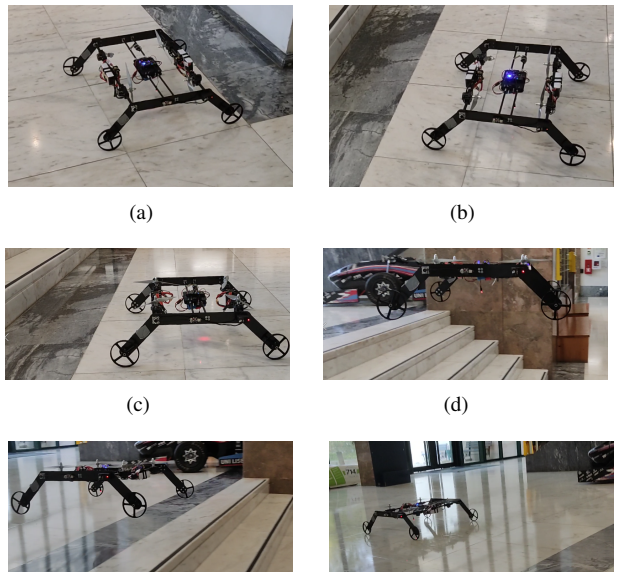

(a) (b)

(c) (d)

(e) (f)

Fig. 15. Demonstration of the multi-modal capabilities of BogieCopter: (a) Start of the ground locomotion (b) MAV facing an obstacle (c) Change to flight mode (d) - (e) Flying to overcome obstacle (f) Once obstacle is surpassed, change back to more efficient ground mode

edge, the ability to move on inclined surfaces by a multi-modal MAV has only been theorized in [29] and demonstrated in [31], by showing the MAV climbing stairs. Due to the design of BogieCopter, the behaviour of the MAV while climbing inclined surfaces should be similar to the one that the vehicle exhibits when moving on flat surfaces. Furthermore, *a priori* knowledge of the slope angle isn't required for an efficient locomotion. Tests were conducted to validate the performance of BogieCopter on inclined surfaces. Multiple inclined surfaces were tested, from low slope angles of 2° up to medium slope angles of 33°. Figure 16 shows BogieCopter climbing a 33° inclined surface.

(a) (b)

Fig. 16. Test on 33° inclined surface: (a) Start of the climb (b) Reaching the top of the inclined surface

Wall-Climbing: As mentioned in subsection III-B, the design of BogieCopter should enable it to wall-climb, similarly to [12]. This ability can have benefits for several applications [12], opening up a new range of possibilities for the developed MAV. A test was conducted to validate this assumption, being the results depicted in figure 17. This test was conducted with the rotors of the vehicle tilted at an angle of 135°, being possible to demonstrate the wall-climb capability of the MAV.

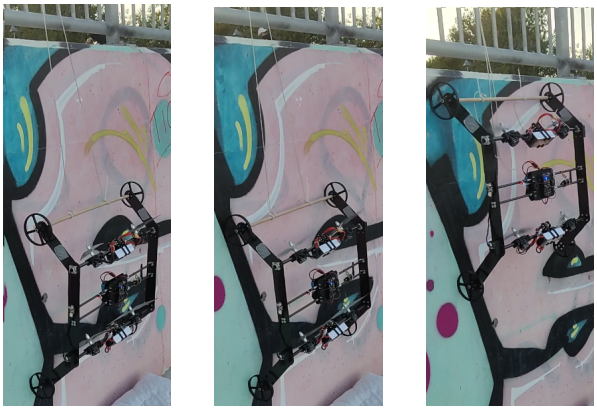

(a) (b) (c)

Fig. 17. Test the capabilities of BogieCopter to wall-climb: (a) Developed MAV being suspended close to a wall by a rope (rope in tension) (b) MAV sticking to the wall, due to the downforce created by the rotors (c) MAV climbing the wall (notice that the rope is no longer in tension

D. Power Consumption

During all the performed tests with BogieCopter, the instantaneous current and battery voltage were logged, enabling an analysis of the required power consumption to maintain each operating state. Figure 18 presents these power consumptions.

The power mode, presented in figure 18, is a mode in which the four rotors are used to climb the inclined surface, instead of two, as with the usual ground mode.

By analysing figure 18, it is possible to verify that, as expected, the ground locomotion on flat surfaces is the operating

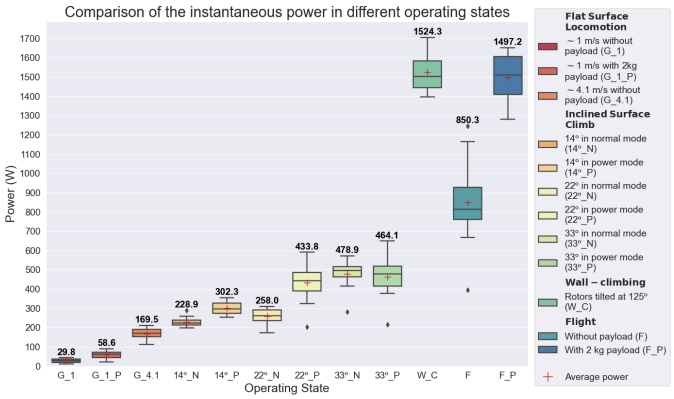

Fig. 18. Comparison between the power required to maintain each operating state. The value above the box plots corresponds to the average power consumption

state that requires less energy. In fact, comparing the flight without payload to the ground locomotion without payload, at 1 m/s, the latter one requires 28.8x less energy than the first one, only requiring 29.8 W. To the best of our knowledge, this is the lowest (best) value among multi-modal MAVs for these weighs, being even better than the required power consumption of active actuated designs. The locomotion modes with a 2 kg payload require, approximately, 2 times more energy than the correspondent modes without payload. Moving on the ground with a 2 kg payload at 1 m/s, only requires 58.6 W, 25.5x less than flying with the payload. Considering the batteries currently being used in BogieCopter, the vehicle is able to achieve an operating distance of $\sim$ 11.5 km while moving on flat surfaces at 1 m/s and $\sim$ 8.2 km while moving at 4.1 m/s.

As expected, the power required to remain on an inclined surface increases with the increase of the surface's slope, being, still, more efficient than the hovering state. The power mode required, usually, more energy than the correspondent normal mode. This has to do with the position of the rotors, which makes the backward rotors work in the wake of the front rotors, having the same performance as co-axial rotors, with the higher power consumption.

A power consumption that wasn't expected is the one for the wall-climb operating state (without payload). This was even higher than the flight operating state with the 2 kg payload. This result can be the result of the operation of the vehicle without the optimized tilt of the rotors, as demonstrated in [12]. This will be further investigated in the future.

VI. Conclusion

This research presents the design, development and test of a passive actuated multi-modal MAV, BogieCopter, which solves the design issues of prior work in the area. One of the design constraints of the developed vehicle was related to the payload capacity, which should be high enough for the vehicle to be used in most inspection applications, having been achieved. BogieCopter can offer several benefits for multiple applications that make use of MAVs (besides inspection), due to its multi-modality, offering extended operating times when used in ground mode (for example, surveillance while perched). Besides the development of a real prototype, in this work, simulator models were also created, easing the continuous development of the platform in a simulated environment. The capabilities of BogieCopter were demonstrated throughout a multitude of tests, including: flight, flat and inclined surfaces locomotion, multi-modality, and even wall-climb tests. To the best of our knowledge, BogieCopter is the MAV with the lowest percentage of mass for the ground actuation mechanism on the MTOM, considering only designs that don't require active actuation to be static on flat surfaces. It is also the one with the highest payload capacity, considering the same T/W ratio for all the prior designs, and is the design with the lowest power consumption while moving on the ground.

VII. Future Work

Despite BogieCopter being a proof-of-concept, the prototype can be further improved, with simple modifications, greatly increasing its capabilities. The CFRP components can be optimized for the design load cases, reducing the total mass of the vehicle and the rotors can be changed for the more efficient ones. These two modifications can greatly increase the operating time of the vehicle. Besides modifications to the hardware, the firmware can be improved and energy aware path algorithms can be explored. Furthermore, the capabilities of BogieCopter can be further expanded, by exploring the wall-climb features, hovering at any given pitch angle, the water locomotion capability of the prototype, and the more efficient forward flight that can be achieved by the use of tilt rotors. The design of the wheels can also be analysed, through multiple tests, to identify the optimal material and wheel's size. Finally, overall, BogieCopter's performance can be evaluated in real inspection applications.

References

[1] S. Herwitz, L. Johnson, S. Dunagan, R. Higgins, D. Sullivan, J. Zheng, B. Lobitz, J. Leung, B. Gallmeyer, M. Aoyagi, R. Slye, and J. Brass, "Imaging from an unmanned aerial vehicle: agricultural surveillance and decision support," *Computers and Electronics in Agriculture*, vol. 44, no. 1, pp. 49–61, 2004.

[2] M. Burri, J. Nikolic, C. Hürzeler, G. Caprari, and R. Siegwart, "Aerial service robots for visual inspection of thermal power plant boiler systems," in *2012 2nd International Conference on Applied Robotics for the Power Industry (CARPI)*, 2012, pp. 70–75.

[3] A.-a. Agha-mohammadi, N. K. Ure, J. P. How, and J. Vian, "Health aware stochastic planning for persistent package delivery missions using quadrotors," in *2014 IEEE/RSJ International Conference on Intelligent Robots and Systems*, 2014, pp. 3389–3396.

[4] S. Waharte and N. Trigoni, "Supporting search and rescue operations with uavs," in *2010 International Conference on Emerging Security Technologies*, 2010, pp. 142–147.

[5] A. Lacaze, "Pegasus transforming uav/ugv hybrid vehicle," in *NDIA Ground Vehicle Systems Engineering And Technology Symposium—Autonomous Ground Systems (AGS) Technical Session, Novi, MI*, 2017.

[6] B. Arbanas, A. Ivanovic, M. Car, T. Haus, M. Orsag, T. Petrovic, and S. Bogdan, "Aerial-ground robotic system for autonomous delivery tasks," in *2016 IEEE International Conference on Robotics and Automation (ICRA)*, 2016, pp. 5463–5468.

[7] A. Pretto, S. Aravecchia, W. Burgard, N. Chebrolu, C. Dornhege, T. Falck, F. V. Fleckenstein, A. Fontenla, M. Imperoli, R. Khanna, and et al., "Building an aerial–ground robotics system for precision farming: An adaptable solution," *IEEE Robotics & Automation Magazine*, vol. 28, no. 3, p. 29–49, Sep 2021.

[8] "Factor of safety." [Online]. Available: https://en.wikipedia.org/wiki/Factor_of_safety

[9] Y. Qin, Y. Li, X. Wei, and F. Zhang, "Hybrid aerial ground locomotion with a single passive wheel," *CoRR*, vol. abs/2003.09242, 2020. [Online]. Available: https://arxiv.org/abs/2003.09242

[10] Y. Qin, W. Xu, A. Lee, and F. Zhang, "Gemini: A compact yet efficient bi-copter uav for indoor applications," *IEEE Robotics and Automation Letters*, vol. 5, no. 2, pp. 3213–3220, 2020.

[11] D. D. Fan, R. Thakker, T. Bartlett, M. B. Miled, L. Kim, E. Theodorou, and A.-a. Agha-mohammadi, "Autonomous hybrid ground/aerial mobility in unknown environments," in *2019 IEEE/RSJ International Conference on Intelligent Robots and Systems (IROS)*, 2019, pp. 3070–3077.

[12] W. Myeong and H. Myung, "Development of a wall-climbing drone capable of vertical soft landing using a tilt-rotor mechanism," *IEEE Access*, vol. 7, pp. 4868–4879, 2019.

[13] K. Kawasaki, Y. Motegi, M. Zhao, K. Okada, and M. Inaba, "Dual connected bi-copter with new wall trace locomotion feasibility that can fly at arbitrary tilt angle," in *2015 IEEE/RSJ International Conference on Intelligent Robots and Systems (IROS)*, 2015, pp. 524–531.

[14] N. Meiri and D. Zarrouk, "Flying STAR, a Hybrid Crawling and Flying Sprawl Tuned Robot," in *2019 International Conference on Robotics and Automation (ICRA)*, 2019, pp. 5302–5308.

[15] A. Kalantari, T. Touma, L. Kim, R. Jitosho, K. Strickland, B. T. Lopez, and A.-A. Agha-Mohammadi, "Drivocopter: A concept hybrid aerial/ground vehicle for long-endurance mobility," in *2020 IEEE Aerospace Conference*, 2020, pp. 1–10.

[16] W. Mielniczek, "B-unstoppable all terrain tank-quadcopter drone," 2015. [Online]. Available: https://www.kickstarter.com/projects/2017062404/b-unstoppable

[17] S. Morton and N. Papanikolopoulos, "A small hybrid ground-air vehicle concept," in *2017 IEEE/RSJ International Conference on Intelligent Robots and Systems (IROS)*, 2017, pp. 5149–5154.

[18] K. Tanaka, D. Zhang, S. Inoue, R. Kasai, H. Yokoyama, K. Shindo, K. Matsuhiro, S. Marumoto, H. Ishii, and A. Takanishi, "A design of a small mobile robot with a hybrid locomotion mechanism of wheels and multi-rotors," in *2017 IEEE International Conference on Mechatronics and Automation (ICMA)*, 2017, pp. 1503–1508.

[19] W. Wang, C. y. Li, L. h. Chu, and C. y. Qu, "Study on air-ground amphibious agricultural information collection robot," in *2016 13th International Conference on Ubiquitous Robots and Ambient Intelligence (URAI)*, 2016, pp. 938–944.

[20] A. R S and M. M. Dharmana, "Multi-terrain multi-utility robot," *Procedia Computer Science*, vol. 133, pp. 651–659, 2018, international Conference on Robotics and Smart Manufacturing (RoSMa2018).

[21] JJRC, "H3." [Online]. Available: https://www.geekbuying.com/item/JJRC-H3-Air-Ground-Airphibian-2-4G-4-Channel-6-Axis-Gyro-RC-Quadcopter-with-2-0MP-Camera-Four-Wheel-UFO---Blue-343423.html

[22] Syma, "X9." [Online]. Available: https://www.dhgate.com/product/syma-x9-air-land-dual-mode-rc-flying-car/373183748.html

[23] A. Kalantari and M. Spenko, "Design and experimental validation of hytaq, a hybrid terrestrial and aerial quadrotor," in *2013 IEEE International Conference on Robotics and Automation*, 2013, pp. 4445–4450.

[24] ——, "Modeling and performance assessment of the hytaq, a hybrid terrestrial/aerial quadrotor," *IEEE Transactions on Robotics*, vol. 30, no. 5, pp. 1278–1285, 2014.

[25] M. Yamada, M. Nakao, Y. Hada, and N. Sawasaki, "Development and field test of novel two-wheeled uav for bridge inspections," in *2017 International Conference on Unmanned Aircraft Systems (ICUAS)*, 2017, pp. 1014–1021.

[26] K. Kawasaki, M. Zhao, K. Okada, and M. Inaba, "Muwa: Multi-field universal wheel for air-land vehicle with quad variable-pitch propellers," in *2013 IEEE/RSJ International Conference on Intelligent Robots and Systems*, 2013, pp. 1880–1885.

[27] S. Mizutani, Y. Okada, C. J. Salaan, T. Ishii, K. Ohno, and S. Tadokoro, "Proposal and experimental validation of a design strategy for a uav with a passive rotating spherical shell," in *2015 IEEE/RSJ International Conference on Intelligent Robots and Systems (IROS)*, 2015, pp. 1271–1278.

[28] S. Sabet, A.-A. Agha-Mohammadi, A. Tagliabue, D. S. Elliott, and P. E. Nikravesh, "Rollocopter: An energy-aware hybrid aerial-ground mobility for extreme terrains," in *2019 IEEE Aerospace Conference*, 2019, pp. 1–8.

[29] A. Tagliabue, S. Schneider, M. Pavone, and A. Agha-mohammadi, "Shapeshifter: A multi-agent, multi-modal robotic platform for exploration of titan," *CoRR*, vol. abs/2002.00515, 2020. [Online]. Available: https://arxiv.org/abs/2002.00515

[30] A. Agha-mohammadi, A. Tagliabue, S. Schneider, B. Morrell, M. Pavone, J. Hofgartner, I. A. D. Nesnas, R. B. Amini, A. Kalantari, A. Babuscia, and J. I. Lunine, "The shapeshifter: a morphing, multi-agent, multi-modal robotic platform for the exploration of titan (preprint version)," *CoRR*, vol. abs/2003.08293, 2020. [Online]. Available: https://arxiv.org/abs/2003.08293

[31] N. Takahashi, S. Yamashita, Y. Sato, Y. Kutsuna, and M. Yamada, "All-round two-wheeled quadrotor helicopters with protect-frames for air–land–sea vehicle (controller design and automatic charging equipment)," *Advanced Robotics*, vol. 29, no. 1, pp. 69–87, 2015.

[32] Parrot, "Rolling Spider," 2014. [Online]. Available: https://www.amazon.com/Parrot-PF723000-ROLLING-SPIDER/dp/B00KZM53NC

[33] Inkonova, "Tilt Scout," 2018. [Online]. Available: https://dronemajor.net/brands/inkonova/products/tilt-scout

[34] J. R. Page and P. E. I. Pounds, "The quadroller: Modeling of a uav/ugv hybrid quadrotor," in *2014 IEEE/RSJ International Conference on Intelligent Robots and Systems*, 2014, pp. 4834–4841.

[35] L. J. Gordon, *Principles of Helicopter Aerodynamics*, 2^{nd} ed., ser. Cambridge Aerospace Series. New York: Cambridge University Press, 2006.

[36] B. Theys, G. Dimitriadis, P. Hendrick, and J. De Schutter, "Influence of propeller configuration on propulsion system efficiency of multi-rotor unmanned aerial vehicles," in *2016 International Conference on Unmanned Aircraft Systems (ICUAS)*, 2016, pp. 195–201.

[37] S. Bouabdallah, "Design and control of quadrotors with application to autonomous flying," Ph.D. dissertation, École Polytechnique Fédérale de Lausanne, February 2007.

[38] G. Hoffmann, H. Huang, S. Waslander, and C. Tomlin, "Quadrotor helicopter flight dynamics and control: Theory and experiment," in *AIAA guidance, navigation and control conference and exhibit*, 2007, p. 6461.

[39] R. M. DeSantis, "Modeling and path-tracking control of a mobile wheeled robot with a differential drive," *Robotica*, vol. 13, no. 4, p. 401–410, 1995.

[40] T. J. de Vries, C. van Heteren, and L. Huttenhuis, "Modeling and control of a fast moving, highly maneuverable wheelchair," in *Proceedings of the International Biomechatronics workshop*, no. April, 1999, pp. 110–115.

[41] R. Dhaouadi and A. A. Hatab, "Dynamic modelling of differential-drive mobile robots using lagrange and newton-euler methodologies: A unified framework," *Advances in Robotics & Automation*, vol. 2, no. 2, pp. 1–7, 2013.

[42] M. V. Pimentel, "Design and control of a bimodal aerial robot for locomotion in flat and inclined surfaces," Master's thesis, Instituto Superior Técnico, April 2021.

[43] K. Xiao, Y. Meng, X. Dai, H. Zhang, and Q. Quan, "A lifting wing fixed on multirotor uavs for long flight ranges," 2020.

[44] K. P. Valavanis, "Advances in unmanned aerial vehicles: state of the art and the road to autonomy," 2008.

[45] C. Ampatis and E. Papadopoulos, "Parametric design and optimization of multi-rotor aerial vehicles," in *2014 IEEE International Conference on Robotics and Automation (ICRA)*, 2014, pp. 6266–6271.

[46] M. Biczyski, R. Sehab, J. F. Whidborne, G. Krebs, and P. Luk, "Multirotor sizing methodology with flight time estimation," *Journal of Advanced Transportation*, vol. 2020, 2020.

[47] G. Hawkins, "F450 dimensions," 2019. [Online]. Available: https://george-hawkins.github.io/arf-drone/docs/f450-dimensions

[48] "APC propellers performance data." [Online]. Available: https://www.apcprop.com/technical-information/performance-data/

[49] F. Kendoul, I. Fantoni, and R. Lozano, "Modeling and control of a small autonomous aircraft having two tilting rotors," *IEEE Transactions on Robotics*, vol. 22, no. 6, pp. 1297–1302, 2006.

[50] S. S. B. System, "Smart Battery Data Specification, Revision 1.1." [Online]. Available: http://sbs-forum.org/specs/sbdat110.pdf

[51] "ArduPilot." [Online]. Available: https://ardupilot.org/

[52] Robotis, "DYNAMIXEL Protocol 1.0." [Online]. Available: https://emanual.robotis.com/docs/en/dxl/protocol1/

[53] F. Furrer, M. Burri, M. Achtelik, and R. Siegwart, *RotorS—A Modular Gazebo MAV Simulator Framework*. Cham: Springer International Publishing, 2016, pp. 595–625.